Coordinated Multi-Point Transmissions Based On Interference Alignment and Neutralization

Zhao Li[*†], Sha Cui[*], Kang G. Shin[†], Jun Gu[*]

[*]State Key Laboratory of Integrated Service Networks, Xidian University
[†]Department of Electrical Engineering and Computer Science, The University of Michigan
zli@xidian.edu.cn, scui4956@gmail.com, kgshin@eecs.umich.edu, gujun1989@126.com

Abstract—**Both interference alignment (IA) and interference neutralization (IN) are exploited for Coordinated Multi-Point (CoMP) transmissions. With the base station's cooperation, transmit precoder and receive filter are designed jointly, and then concurrent transmissions of multiple data streams are achieved. In the design of preprocessing, IN is applied to the interferences carrying same data so as to align the interfering signals with opposite directions in a subspace. On the other hand, for interferences carrying different information, IA is employed to align them with the same direction in a subspace, thus reducing the interference signal dimension observed at the user side. Based on different precoding schemes at the transmitter's side, receivers adopt zero-forcing (ZF) so as to recover the desired data. The proposed *interference alignment and neutralization based CoMP* (IAN-CoMP) mechanism can achieve effective interference cancellation and suppression by exploiting limited and flexible collaboration only at the base station (BS) side. We also extend the mechanism to general cases where the antenna configurations at both transmitter and receiver side, the number of transmitters participating in CoMP and simultaneously served users are variable. In addition, the proposed scheme can also achieve a flexible tradeoff between cooperation overhead and the system's achievable degrees of freedom (DoFs). Our in-depth simulation results show that IAN-CoMP can significantly improve the spectral efficiency (SE) for cell-edge users.**

I. Introduction

Improving spectral efficiency to meet the rapidly growing demand for high-speed data transmission is of great importance to wireless communication service providers [1]. In particular, as the frequency reuse efficiency improves, cell-edge users suffer more co-channel interference (CCI) from adjacent cells, which degrades the overall system performance. Therefore, how to solve the interference problem for cell-edge users and improve the system throughput becomes a critical issue. Coordinated multi-point (CoMP) transmission—designed to solve the problem by enforcing the cooperation of multiple cells—is a promising technique and has been chosen as a key technology in the 3rd Generation Partnership Project (3GPP) long-term evolution-advanced (LTE-A) systems [2-3].

Besides CoMP, there are other types of interference management, such as zero-forcing (ZF) [4-6] and interference alignment (IA) [7-9]. By using these, a set of BSs jointly encode transmit symbols, so that interference at the receiver may be effectively suppressed or mitigated, and then the desired signal is recovered accurately. Thanks to its simplicity, ZF-based precoding has been widely applied to CoMP systems [4-6]. In [4], a hybrid cooperative downlink transmission and preprocessing scheme incorporating JP and CS/CB was proposed for heterogeneous networks. In [5], a low-feedback scheduling scheme was proposed for downlink CoMP systems, in which multiple users are selected and then served with zero-forcing beamformer simultaneously by several cooperative BSs. In [6], a dynamic switching mechanism between CoMP mode and non-CoMP mode was proposed to adapt to a dynamically changing communication environment.

IA is a novel interference management technique that has been under development in recent years [7-9]. By pre-processing at the transmitter, multiple interfering signals are mapped into a finite subspace, i.e., the overall interference space at the destination/receiver is minimized, so that the desired signal(s) may be sent through a subspace without attenuation. The authors of [7] showed that the feasibility of IA is highly dependent on system parameters, such as the numbers of transmitters and receivers, configuration of transmit/receive antennas, etc. IA-based beamforming was proposed in [8] to improve the downlink performance of multiple cell-edge users in multi-user MIMO (Multiple-input multiple-output) systems. A CoMP mechanism incorporated with IA was proposed in [9] for multi-cell multi-user downlink systems based on partial information exchange where both IA and successive decoding are employed. Although this method can improve system throughput, it is based on the user side cooperation which is impractical due to the limited capability of, and the overhead at mobile terminals, non-interoperability between different operators, etc.

For wireless networks, interference can be not only aligned but also canceled or partially canceled through multiple paths, which is referred to as *interference neutralization* (IN) [10-13]. IN seeks to properly combine signals arriving from various paths in such a way that the interfering signals are canceled while the desired signals are preserved [10]. It can be regarded as a distributed zero forcing of interference [11], i.e., transmissions from separate sources cancel each other at a destination without either source actually forming a null to the destination. Note that in practical communications, the interfering transmitters may have their own transmission demands, i.e., the data from multiple transmitters are always different. So, how to incorporate data transmission with interference elimination is a critical issue in the IN-based mechanism design. The authors of [10] constructed

a linear distributed IN scheme that encodes in both space and time for separated multiuser uplink-downlink two-way communications. In [11], an aligned IN was proposed in a multi-hop interference network formed by concatenation of two two-user interference channels. The mechanism provides a way to align interference terms over each hop in a manner that allows them to be canceled over the air at the last hop. In [12-13], instantaneous relay (relay-without-delay) was introduced to achieve a higher capacity than conventional relays. With those schemes, relays receive desired and interference signals from source nodes and reconstruct them before forwarding to the destinations so as to achieve partial interference elimination (i.e., IN) at the destinations and preserve the desired signal. Although the studies based on instantaneous relay can provide some useful theoretical results, this type of relay is too idealistic. In addition, most of the existing work [10-13] investigated IN in multi-hop interference relay channels. By exploiting the broadcast feature of wireless communications, relay nodes receive both desired and interference signals, then apply proper signal reconstruction to implement IN at the destination. However, dedicated relay nodes are needed, which may increase the system cost and complexity. Moreover, in some practical cases, relays may not be necessary.

Motivated by the above observations, we exploit the cooperative capability of eNBs (or eNodeBs) in LTE system to propose a CoMP mechanism incorporating both IA and IN (IAN-CoMP). With IAN-CoMP, data symbols are properly assigned to collaborating eNBs, and precoding and filtering algorithms are jointly designed, so that concurrent transmissions of multiple data streams is achieved.

The contributions of this paper are two-fold:

- A CoMP transmission scheme based on *interference alignment and neutralization* is proposed. Both IN and IA are employed for appropriately adjusting interfering signals carrying identical and different information, respectively.
- The proposed scheme is extended to general cases where the number of antennas at both transmitter and receiver, the number of eNBs participating in CoMP and simultaneously served UEs are variable. Moreover, it could acquire a flexible tradeoff between cooperation overhead and achievable DoFs.

In this paper, the terminology DoF is defined by the number of concurrent interference-free data streams the system can support. Throughout this paper, we use the following notations. The set of complex numbers is denoted as $\mathbb{C}$, while vectors and matrices are represented by bold lower-case and upper-case letters, respectively. Let $\mathbf{X}^H$, $\mathbf{X}^{-1}$, and $det(\mathbf{X})$ denote the Hermitian, inverse, and determinant of matrix $\mathbf{X}$. $\|\cdot\|$ indicates the Euclidean norm. $E(\cdot)$ denotes statistical expectation. $\langle \mathbf{a}, \mathbf{b} \rangle$ represents the inner product of two vectors.

II. SYSTEM MODEL

Let's consider a CoMP system [14] consisting of a cluster of adjacent cells as shown in Fig. 1. Downlink transmission is considered. We use M and L to denote the numbers of eNBs

and UEs, respectively. The number of antennas at each base station, i.e., eNB_i $(i = 1, 2, \cdots, M)$ is N_T. The eNBs operate in a synchronized slot structure. In each time slot, eNB allocates different resource block to its UEs, so that CCI within a cell is avoided. UEs are randomly distributed in the network. For clarity, only three UEs are clearly plotted of which two are located in the overlapping area of two cells whereas the other one lies in the central area of a cell. The unclear UEs in Fig. 1 indicate those are not scheduled in the current slot. The number of antennas at each UE_j $(j = 1, 2, \cdots, L)$ is N_R. We assume that UE_1 is affiliated with eNB_1 whereas eNB_2 and eNB_3 are the home BSs for UE_2 and UE_3, respectively. For cell-edge users, they would suffer CCI from adjacent eNBs. As for the central area UEs, they will be directly served by their home eNBs without interference. In this paper, we focus on the design of downlink cooperative transmission aiming to improve edge users' communication performance. For clarity of exposition, we begin our design in a specific case in which two eNBs and two UEs, each of them is equipped with two antennas ($N_T = N_R = 2$), are included. Then in Section IV the proposed scheme is extended to generalized situations.
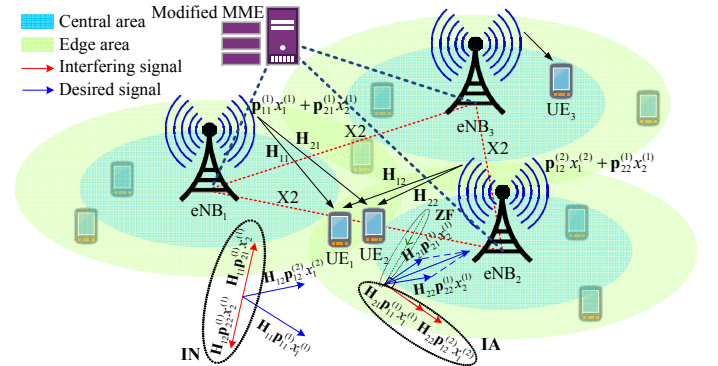

Fig. 1. System model.

No cooperation is available between UEs. Let $\mathbf{H}_{ji} \in \mathbb{C}^{N_R \times N_T}$ be the channel matrix from eNB_i to UE_j. A spatially uncorrelated Rayleigh flat fading channel model is assumed so that the elements of $\mathbf{H}_{ji}$ are modeled as independent and identically distributed zero-mean unit-variance complex Gaussian random variables. All users experience block fading, i.e., channel parameters in a block consisting of several successive transmission cycles remain constant in the block and vary randomly between blocks. The eNBs can acquire channel state information (CSI) accurately via users' feedback, and share users' data or/and CSI with other eNBs via X2 interface or a modified MME (Mobility management entity). We assume the backhaul dedicated to CSI, data information, and signaling delivery are reliable, with which the latency could be reduced to low, even negligible levels relative to the time scale on which the channel state varies [15-16]. The transmit power of each eNB, denoted by P_T, is equally distributed over the eNB's transmitted data streams.

III. IAN-BASED CoMP TRANSMISSION

In this section, we detail an IAN-based CoMP mechanism under specific system settings where $M = 2$, $L = 2$, and

$N_T = N_R = 2$, with which 3 data streams can be simultaneously supported. We assume that UE$_1$ is assigned to 2 streams, denoted by $x_1^{(1)}$ and $x_1^{(2)}$, respectively, while UE$_2$ is served with a single data stream $x_2^{(1)}$. Due to the symmetrical feature of the system model, if UE$_1$ is served by one stream and UE$_2$ by two, the proposed scheme is directly applicable. Although the method based on interference alignment and cancellation (IAC) [17] can also achieve the same number of concurrent data streams with an identical system configuration, it requires receiver-side collaboration which is impractical to downlink communications. Moreover, the proposed IAN-based strategy only needs partial users' data sharing between eNBs. Specifically, eNB$_1$ *transfers* an arbitrary data stream to be sent to UE$_1$, say $x_1^{(2)}$ to eNB$_2$, whereas for the data intended for UE$_2$, i.e., $x_2^{(1)}$, it is *shared* between eNB$_2$ and eNB$_1$, then both eNBs transmit $x_2^{(1)}$ to UE$_2$ cooperatively. According to the above description, each eNB precodes and transmits two data streams to two UEs, as shown in Fig. 1. On one hand, IN is used to adjust two interfering signals of the same data in opposite directions in a subspace such that they can be neutralized at a target UE. On the other hand, IA is applied to align interference signals carrying different information in the same direction in a subspace to reduce the received signal dimension. Based on the cooperative preprocessing at eNBs, ZF is employed at each UE to cancel the residual interference and recover the desired data.

A. IAN-Based Transmit Precoding Design

The mixed signal received at UE$_1$ and UE$_2$ can be expressed, respectively, as Eqs. (1) and (2) below:

$$\mathbf{y}_1 = \mathbf{H}_{11}\mathbf{p}_{11}^{(1)}x_1^{(1)} + \mathbf{H}_{12}\mathbf{p}_{12}^{(2)}x_1^{(2)} + \left(\mathbf{H}_{11}\mathbf{p}_{21}^{(1)} + \mathbf{H}_{12}\mathbf{p}_{22}^{(1)}\right)x_2^{(1)} + \mathbf{z}_1$$

$$(1)$$

$$\mathbf{y}_2 = \left(\mathbf{H}_{21}\mathbf{p}_{21}^{(1)} + \mathbf{H}_{22}\mathbf{p}_{22}^{(1)}\right)x_2^{(1)} + \mathbf{H}_{21}\mathbf{p}_{11}^{(1)}x_1^{(1)} + \mathbf{H}_{22}\mathbf{p}_{12}^{(2)}x_1^{(2)} + \mathbf{z}_2$$

$$(2)$$

where $\mathbf{H}_{ji} \in \mathbb{C}^{2\times 2}$ $(i, j = 1, 2)$. The transmit symbols to UE$_1$ and UE$_2$ are denoted by $x_1^{(m)}$ $(m = 1, 2)$ and $x_2^{(1)}$, respectively. Here we use the terminologies *data symbol* and *data stream* to mean the same since the latter can be regarded as a continuous process of symbol transmission. Moreover, the analysis in this paper is based on a discrete-time process where the time index is omitted for simplicity. $\mathbf{p}_{ji}^{(m)} \in \mathbb{C}^{N_T \times 1}$ is the precoding vector that eNB$_i$ adopts for data $x_j^{(m)}$ to transmit to UE$_j$.

The first two terms on the right hand side (RHS) of Eq. (1) indicate the expected signal for UE$_1$, whereas the third term denotes the interference caused by the transmission of shared data $x_2^{(1)}$ from two collaborating eNBs to UE$_2$. The first term on the RHS of Eq. (2) represents the expected transmission to UE$_2$, whereas the second and third terms denote the interference caused by the transmission of $x_1^{(1)}$ from eNB$_1$ to UE$_1$ and $x_1^{(2)}$ from eNB$_2$ to UE$_1$, respectively. $\mathbf{z}_j \in \mathbb{C}^{N_R \times 1}$ is an additive white Gaussian noise (AWGN) vector whose elements have zero-mean and variance σ_n^2. $E(\mathbf{z}_j\mathbf{z}_j^H) = \sigma_n^2\mathbf{I}_{N_R}$,

where $\mathbf{I}_{N_R}$ is an $N_R \times N_R$ identity matrix. Based on the above description, both eNBs send $x_2^{(1)}$ to UE$_2$, i.e., $x_2^{(1)}$ is *shared* by two eNBs. As for UE$_1$, its intended data $x_1^{(1)}$ and $x_1^{(2)}$ are precoded and transmitted by two eNBs, respectively, i.e., one data is *transferred* from eNB$_1$ to eNB$_2$. Therefore, $E(\|x_1^{(m)}\|^2) = P_T/2$ $(m = 1, 2)$, $E(\|x_2^{(1)}\|^2) = P_T/2$.

From Eq. (1), one can see that two interfering signals carry same data $x_2^{(1)}$, so that joint precoding can be designed to achieve IN at UE$_1$. As for (2), there are two different interferences carrying $x_1^{(1)}$ and $x_1^{(2)}$, respectively. Hence, IA is employed to align the interferences in one direction at UE$_2$. Then, UE$_2$ can implement ZF to cancel the aligned interference and recover its expected information (see Section III.B for details). It should be noted that the direction in which two interferences align at UE$_2$ may be optimized to enhance transmission performance. Due to limited space, we only investigate the alignment based on the subspace determined by $\mathbf{H}_{21}\mathbf{p}_{11}^{(1)}$ or $\mathbf{H}_{22}\mathbf{p}_{12}^{(2)}$.

The precoding vectors designed for eNB should therefore meet the following conditions:

$$\mathbf{H}_{11}\mathbf{p}_{21}^{(1)} + \mathbf{H}_{12}\mathbf{p}_{22}^{(1)} = \mathbf{0}, \quad \mathbf{H}_{21}\mathbf{p}_{11}^{(1)} = \mathbf{H}_{22}\mathbf{p}_{12}^{(2)} \qquad (3)$$

We can then obtain:

$$\mathbf{p}_{22}^{(1)} = -\mathbf{H}_{12}^{-1}\mathbf{H}_{11}\mathbf{p}_{21}^{(1)}, \quad \mathbf{p}_{12}^{(2)} = \mathbf{H}_{22}^{-1}\mathbf{H}_{21}\mathbf{p}_{11}^{(1)} \qquad (4)$$

The second equation in Eq. (4) is to design $\mathbf{p}_{12}^{(2)}$ such that $\mathbf{H}_{22}\mathbf{p}_{12}^{(2)}$ aligns in the direction determined by $\mathbf{H}_{21}\mathbf{p}_{11}^{(1)}$. Similarly, we can also design $\mathbf{p}_{11}^{(1)} = \mathbf{H}_{21}^{-1}\mathbf{H}_{22}\mathbf{p}_{12}^{(2)}$ so as to make $\mathbf{H}_{21}\mathbf{p}_{11}^{(1)}$ align in the subspace determined by $\mathbf{H}_{22}\mathbf{p}_{12}^{(2)}$. For a concise analysis, we introduce equivalent matrices $\mathbf{G}_1 = \mathbf{H}_{22}^{-1}\mathbf{H}_{21}$ and $\mathbf{G}_2 = \mathbf{H}_{12}^{-1}\mathbf{H}_{11}$. Then a general form of precoder, $\mathbf{p}_{j2}^{(m)} = (-1)^m\mathbf{G}_j\mathbf{p}_{j1}^{(1)}$ where $(m, j) \in \{(1, 2), (2, 1)\}$, is obtained. Note that when antenna configurations are generalized (see Section IV.A for detail), the inverse of channel matrix should be replaced by Moore-Penrose pseudo-inverse so as to calculate the precoders.

From the above general expression we can see that in order to calculate $\mathbf{p}_{j2}^{(m)}$, $\mathbf{p}_{j1}^{(1)}$ should be determined first. Applying the singular value decomposition (SVD) to $\mathbf{H}_{j1}$ $(j = 1, 2)$, we get $\mathbf{H}_{j1} = \mathbf{U}_{j1}\mathbf{D}_{j1}\mathbf{V}_{j1}^H$ where $\mathbf{U}_{j1} = [\mathbf{u}_{j1}^{(1)} \ \mathbf{u}_{j1}^{(2)}]$, $\mathbf{D}_{j1} = \begin{bmatrix} \lambda_{j1}^{(1)} & 0 \\ 0 & \lambda_{j1}^{(2)} \end{bmatrix}$ and $\mathbf{V}_{j1} = [\mathbf{v}_{j1}^{(1)} \ \mathbf{v}_{j1}^{(2)}]$. The column vectors of $\mathbf{U}_{j1}$ and $\mathbf{V}_{j1}$ indicate spatial features, whereas non-zero principal diagonal elements of $\mathbf{D}_{j1}$, sorted in descending order, represent for the amplitude gains of a set of decoupled parallel subchannels. In order to achieve as high a transmission rate as possible, we adopt $\mathbf{p}_{j1}^{(1)} = \mathbf{v}_{j1}^{(1)}$, i.e., the principal subchannel with the maximum singular value $\lambda_{j1}^{(1)}$ is selected. Then, Eqs. (1) and (2) can be rewritten as (5) and (6) below:

$$\mathbf{y}_1 = \lambda_{11}^{(1)}\mathbf{u}_{11}^{(1)}x_1^{(1)} + \mathbf{H}_{12}\mathbf{G}_1\mathbf{v}_{11}^{(1)}x_1^{(2)} + \mathbf{z}_1 \qquad (5)$$

$$\mathbf{y}_2 = \left(\lambda_{21}^{(1)}\mathbf{u}_{21}^{(1)} - \mathbf{H}_{22}\mathbf{G}_2\mathbf{v}_{21}^{(1)}\right)x_2^{(1)} + \mathbf{H}_{21}\mathbf{v}_{11}^{(1)}\left(x_1^{(1)} + x_1^{(2)}\right) + \mathbf{z}_2$$

$$(6)$$

Here we should note that although $\mathbf{p}_{j1}^{(1)}$ is a unit vector, $\mathbf{p}_{j2}^{(1)}$ is probably not. Moreover, in order to achieve IN, the two signals should have the same strength and be with opposite direction; whereas for IA, only identical direction is required. As a consequence, $\mathbf{p}_{12}^{(2)}$ should be normalized before using so that neither power gain nor attenuation is introduced. However, $\mathbf{p}_{22}^{(1)}$ cannot be scaled due to the purpose of IN. In practice, we could adjust the signal with a higher channel gain to neutralize the one with lower gain so as to avoid additional power cost.

From Eq. (5) one can see that the interferences caused by the transmission of $x_2^{(1)}$ from eNB$_1$ and eNB$_2$ to UE$_2$ are neutralized at UE$_1$ via IN. Eq. (6) indicates that the interferences caused by sending $x_1^{(1)}$ and $x_1^{(2)}$ from two eNBs to UE$_1$ align in the same direction at UE$_2$ with IA. However, the interference is not eliminated, as shown in (6). Next, we elaborate the design of receive filter to cancel the residual interference and recover the expected information.

B. Design of Receive Filter

In this subsection, ZF is employed to cancel the residual interference and decode the expected data. Note that no user-side collaboration is assumed, so each UE implements post-processing independently.

Adopt $\mathbf{F}_j^H = [\mathbf{f}_j^{(1)}\ \mathbf{f}_j^{(2)}]^H$ to denote the filter matrix of $\mathbf{y}_j$ where $j = 1,2$. For simplicity, let $\mathbf{C}_1^{(1)} = \lambda_{11}^{(1)}\mathbf{u}_{11}^{(1)} = \|\mathbf{C}_1^{(1)}\|\mathbf{u}_{\mathbf{C}_1^{(1)}}$, $\mathbf{C}_1^{(2)} = \mathbf{H}_{12}\mathbf{G}_1\mathbf{v}_{11}^{(1)} = \|\mathbf{C}_1^{(2)}\|\mathbf{u}_{\mathbf{C}_1^{(2)}}$, $\mathbf{C}_2^{(1)} = \lambda_{21}^{(1)}\mathbf{u}_{21}^{(1)} - \mathbf{H}_{22}\mathbf{G}_2\mathbf{v}_{21}^{(1)} = \|\mathbf{C}_2^{(1)}\|\mathbf{u}_{\mathbf{C}_2^{(1)}}$ and $\mathbf{C}_2^{(2)} = \mathbf{H}_{21}\mathbf{v}_{11}^{(1)} = \|\mathbf{C}_2^{(2)}\|\mathbf{u}_{\mathbf{C}_2^{(2)}}$. The amplitude of $\mathbf{C}_j^{(m)}$ is $\|\mathbf{C}_j^{(m)}\|$ whereas $\mathbf{u}_{\mathbf{C}_j^{(m)}} = \mathbf{C}_j^{(m)}/\|\mathbf{C}_j^{(m)}\|$ indicates the direction of $\mathbf{C}_j^{(m)}$. These coefficients are substituted into (5) and (6) and $\mathbf{F}_j^H$ is adopted as the filter to obtain Eqs. (7) and (8).

$$\bar{\mathbf{y}}_1 = \mathbf{F}_1^H\|\mathbf{C}_1^{(1)}\|\mathbf{u}_{\mathbf{C}_1^{(1)}}x_1^{(1)} + \mathbf{F}_1^H\|\mathbf{C}_1^{(2)}\|\mathbf{u}_{\mathbf{C}_1^{(2)}}x_1^{(2)} + \mathbf{F}_1^H\mathbf{z}_1 \quad (7)$$

$$\bar{\mathbf{y}}_2 = \mathbf{F}_2^H\|\mathbf{C}_2^{(1)}\|\mathbf{u}_{\mathbf{C}_2^{(1)}}x_2^{(1)} + \mathbf{F}_2^H\|\mathbf{C}_2^{(2)}\|\mathbf{u}_{\mathbf{C}_2^{(2)}}\left(x_1^{(1)} + x_1^{(2)}\right) + \mathbf{F}_2^H\mathbf{z}_2 \quad (8)$$

Note that $\mathbf{C}_2^{(2)}$ is essentially the coefficient of interference part of the mixed signal received by UE$_2$. The design of receive filter should meet the following condition:

$$\left(\mathbf{f}_j^{(m)}\right)^H\mathbf{u}_{\mathbf{C}_j^{(m')}} = \begin{cases} \alpha_j^{(m)}, & m = m' \\ 0, & m \neq m' \end{cases} \quad (9)$$

where $m, m', j = 1,2$ and $1 \geq \|\alpha_j^{(m)}\| > 0$. Then, the receive filter for UE$_j$ is calculated as:

$$\mathbf{f}_j^{(m)} = \frac{\mathbf{u}_{\mathbf{C}_j^{(m)}} - \mathbf{u}_{\mathbf{C}_j^{(m')}}^H\mathbf{u}_{\mathbf{C}_j^{(m)}}\mathbf{u}_{\mathbf{C}_j^{(m')}}}{\left\|\mathbf{u}_{\mathbf{C}_j^{(m)}} - \mathbf{u}_{\mathbf{C}_j^{(m')}}^H\mathbf{u}_{\mathbf{C}_j^{(m)}}\mathbf{u}_{\mathbf{C}_j^{(m')}}\right\|}, \quad m = m' \quad (10)$$

Substituting (10) into (7) and (8), we get (11) and (12). According to (11), the desired data $x_1^{(1)}$ and $x_1^{(2)}$ of UE$_1$ can be decoded, respectively, in two mutually orthogonal subspaces. As for (12), the expected data $x_2^{(1)}$ of UE$_2$ is recovered in the subspace orthogonal to the one in which residual interference, indicated by the second term on the RHS of (12), is located.

C. Achievable Spectral-Efficiency Analysis

By observing the noise parts in (11) and (12), although co-channel interference is eliminated and the expected data is decoded in an interference-free subspace, $\mathbf{F}_j$ is not a unitary matrix, i.e., $\langle\mathbf{f}_j^{(1)}, \mathbf{f}_j^{(2)}\rangle \neq 0$. As a result, the noise power after receive filtering becomes:

$$E\left\{(\mathbf{F}_j^H\mathbf{z}_j)(\mathbf{F}_j^H\mathbf{z}_j)^H\right\} = E\left\{\mathbf{F}_j^H\mathbf{z}_j\mathbf{z}_j^H\mathbf{F}_j\right\} = \sigma_n^2\mathbf{A}_j \quad (13)$$

where $\mathbf{A}_j = \begin{bmatrix} 1 & (\mathbf{f}_j^{(1)})^H\mathbf{f}_j^{(2)} \\ (\mathbf{f}_j^{(2)})^H\mathbf{f}_j^{(1)} & 1 \end{bmatrix}$.

Given $E(\|x_1^{(m)}\|^2) = P_T/2$ where $m = 1,2$ and $E(\|x_2^{(1)}\|^2) = P_T/2$, The achievable spectral efficiency for each UE is computed as Eqs. (14) and (15). The effect of $\mathbf{A}_j$ on R_1 and R_2 has been studied in [18]. For space limitations we do not discuss it in this paper.

IV. GENERALIZATION OF IAN-COMP

In this section, we extend IAN-CoMP to general cases while varying antenna configurations at both the Tx and Rx sides, the numbers of eNBs participating in CoMP and simultaneously

$$\bar{\mathbf{y}}_1 = \left\|\mathbf{C}_1^{(1)}\right\|\begin{bmatrix} (\mathbf{f}_1^{(1)})^H\mathbf{u}_{\mathbf{C}_1^{(1)}} \\ 0 \end{bmatrix}x_1^{(1)} + \left\|\mathbf{C}_1^{(2)}\right\|\begin{bmatrix} 0 \\ (\mathbf{f}_1^{(2)})^H\mathbf{u}_{\mathbf{C}_1^{(2)}} \end{bmatrix}x_1^{(2)} + \mathbf{F}_1^H\mathbf{z}_1 \quad (11)$$

$$\bar{\mathbf{y}}_2 = \left\|\mathbf{C}_2^{(1)}\right\|\begin{bmatrix} (\mathbf{f}_2^{(1)})^H\mathbf{u}_{\mathbf{C}_2^{(1)}} \\ 0 \end{bmatrix}x_2^{(1)} + \left\|\mathbf{C}_2^{(2)}\right\|\begin{bmatrix} 0 \\ (\mathbf{f}_2^{(2)})^H\mathbf{u}_{\mathbf{C}_2^{(2)}} \end{bmatrix}\left(x_1^{(1)} + x_1^{(2)}\right) + \mathbf{F}_2^H\mathbf{z}_2 \quad (12)$$

$$R_1 = \sum_{m=1}^2 R_1^{(m)} = \sum_{m=1}^2 log_2\left\{det\left[\mathbf{I}_{N_R} + \frac{P_T\left(\mathbf{F}_1^H\mathbf{C}_1^{(m)}\right)\left(\mathbf{F}_1^H\mathbf{C}_1^{(m)}\right)^H}{2\sigma_n^2\mathbf{A}_1}\right]\right\} \quad (14)$$

$$R_2 = log_2\left\{det\left[\mathbf{I}_{N_R} + \frac{P_T\left(\mathbf{F}_2^H\mathbf{C}_2^{(1)}\right)\left(\mathbf{F}_2^H\mathbf{C}_2^{(1)}\right)^H}{2\sigma_n^2\mathbf{A}_2}\right]\right\} \quad (15)$$

served UEs. Before delving into details, we first provide one theorem and three corollaries on IA and IN.

Theorem 1: Each of the signals generated to achieve interference alignment or neutralization at an unintended receiver while being decoded at their intended receiver should be originated from a different transmitter.

Proof sketch: Take the transmission of $x_1^{(1)}$ and $x_1^{(2)}$ as an example, as shown in Fig. 1. If both are sent from eNB_i and aligned in one direction at their unintended receiver UE_2, where $i \in \{1, \cdots, M\}$ is the index of eNB, then $\mathbf{H}_{2i}\mathbf{p}_{2i}^{(1)} = \mathbf{H}_{2i}\mathbf{p}_{2i}^{(2)}$. One can easily see that these two signals also overlap with each other at their intended receiver UE_1, thus becoming indistinguishable. As for IN, if the signal carrying $x_1^{(1)}$ is neutralized at UE_2, then $\mathbf{H}_{2i}\mathbf{p}_{2i}^{(1)}x_1^{(1)} = -\mathbf{H}_{2i}\mathbf{p}_{2i}^{\prime(1)}x_1^{(1)}$, where $\mathbf{p}_{2i}^{\prime(1)}$ represents the precoder for a duplicate signal to mitigate the original interference $\mathbf{H}_{2i}\mathbf{p}_{2i}^{(1)}x_1^{(1)}$ at UE_2. Then, the two signals will also be neutralized at any other UE_j where user index $j \in \{1, \cdots, L\}$ and $j \neq 2$. ∎

Corollary 1: If $\kappa > 1$ interferences are from an identical transmitter, they should be mapped into a κ-dimensional space at their unintended receivers so as to be distinguishable at their intended receiver(s).

Proof sketch: According to Theorem 1, if Corollary 1 is not satisfied, at least two signal components will overlap with each other at a UE, thus becoming indistinguishable. Thus, Corollary 1 follows. ∎

Corollary 2: The same set of signals cannot be simultaneously aligned with each other at more than one receiver.

Proof sketch: Take the transmission of $x_1^{(1)}$ and $x_1^{(2)}$ as an example. According to Theorem 1, they should be sent by two eNBs, say eNB_1 and eNB_2, separately, so as to be aligned in one direction at a UE. Without loss of generality, if two signals carrying $x_1^{(1)}$ and $x_1^{(2)}$ are aligned with each other at UE_1 and UE_2, then $\mathbf{H}_{11}\mathbf{p}_{1i}^{(1)} = \mathbf{H}_{1i'}\mathbf{p}_{1i'}^{(2)}$ and $\mathbf{H}_{2i}\mathbf{p}_{1i}^{(1)} = \mathbf{H}_{2i'}\mathbf{p}_{1i'}^{(2)}$ where $i, i' \in \{1, 2\}$ and $i \neq i'$, should be satisfied simultaneously. Due to the randomness of channel conditions, given $\mathbf{p}_{1i}^{(1)}$ (or $\mathbf{p}_{1i'}^{(2)}$), a solution for the other precoder $\mathbf{p}_{1i'}^{(2)}$ (or $\mathbf{p}_{1i}^{(1)}$), satisfying both equations, usually does not exist. ∎

Similar to Corollary 2, we can derive the following corollary.

Corollary 3: The same pair of signals cannot be neutralized at more than one receiver simultaneously.

Proof sketch: The proof is similar to that in Corollary 2. ∎

In what follows, we extend the proposed IAN-CoMP to more general cases.

A. Generalized Antenna Configurations

The proposed IAN-CoMP can be extended to the general situation in which the antenna configurations at both transmitter and receiver sides are variable. Since mobile stations/devices are subject to severer restrictions such as cost and hardware than a base station, we assume $N_T \geq N_R$. For clarity, our discussion is confined to 2-eNB 2-UE system settings.

Let $\mathbf{s}_1 = [x_1^{(1)} \cdots x_1^{(N_R)}]^T$ and $\mathbf{s}_2 = [x_2^{(1)} \cdots x_2^{(N_R-1)}]^T$ denote the desired data of UE_1 and UE_2, respectively. Vectors $\mathbf{s}_{11} = [x_1^{(1)} \cdots x_1^{(N_R-1)}]^T$ and $\mathbf{s}_2$ are sent by eNB_1, whereas $\mathbf{s}_{12} = [x_1^{(1)} \cdots x_1^{(N_R-2)} x_1^{(N_R)}]^T$ and $\mathbf{s}_2$ are sent by eNB_2. In other words, UE_1's data, except $x_1^{(N_R-1)}$ and $x_1^{(N_R)}$, is *shared* over both eNBs. eNB_1 *transfers* $x_1^{(N_R)}$ to eNB_2 whereas $x_1^{(N_R-1)}$ is sent by eNB_1 exclusively. In addition, both eNBs transmit $\mathbf{s}_2$ to UE_2 cooperatively. In the above description, $x_1^{(N_R-1)}$ and $x_1^{(N_R)}$ are taken as an example in the mechanism design. In practice, any two arbitrary data streams, say $x_1^{(m)}$ and $x_1^{(n)}$ $(m \neq n)$, can be used. Our scheme is still applicable in such cases. For simplicity, an equal power allocation is adopted, i.e., $E(\|x_1^{(m)}\|^2) = E(\|x_2^{(n)}\|^2) = P_T/(2N_R - 2)$ where $m = 1, \cdots, N_R$ and $n = 1, \cdots, N_R - 1$.

Given the above system configurations, the received mixed signal at UE_1 and UE_2 can be expressed as (16) and (17), where $\mathbf{H}_{ji} \in \mathbb{C}^{N_R \times N_T}$ $(i, j = 1, 2)$. $\mathbf{p}_{1i}^{(m)} \in \mathbb{C}^{N_T \times 1}$ $(m = 1, \cdots, N_R)$ is the precoding vector for data $x_1^{(m)}$ that eNB_i transmits to UE_1. $\mathbf{P}_i^{(\mathbf{s}_2)} \in \mathbb{C}^{N_T \times (N_R-1)}$ represents the precoding matrix for $\mathbf{s}_2$ that eNB_i transmits to UE_2. The first three terms on the RHS of (16) indicate the desired signal for UE_1, whereas the fourth term denotes the interference caused by the transmission of shared data $\mathbf{s}_2$ from two cooperating eNBs to UE_2. In (17), the first term on the RHS represents the expected transmission to UE_2, whereas the next three terms denote the interference caused by the transmission of $\mathbf{s}_{11}$ from eNB_1 to UE_1 and $\mathbf{s}_{12}$ from eNB_2 to UE_1, respectively. In (16), two interference signals carry the same data $\mathbf{s}_2$, and hence joint precoding can be adopted to achieve IN at UE_1. In (17), IA is employed to align the interferences in one direction so that the mixed signal's dimension is reduced at UE_2. The precoding vectors designed for eNB should thus meet the following conditions:

$$\begin{cases} \mathbf{H}_{11}\mathbf{P}_1^{(\mathbf{s}_2)} + \mathbf{H}_{12}\mathbf{P}_2^{(\mathbf{s}_2)} = \mathbf{0} \\ \mathbf{H}_{21}\mathbf{p}_{11}^{(m)} + \mathbf{H}_{22}\mathbf{p}_{12}^{(m)} = \mathbf{H}_{21}\mathbf{p}_{11}^{(N_R-1)} = \mathbf{H}_{22}\mathbf{p}_{12}^{(N_R)}. \end{cases} \quad (18)$$

According to Theorem 1, in the second equation of (18), since $\mathbf{H}_{21}\mathbf{p}_{11}^{(N_R-1)} = \mathbf{H}_{22}\mathbf{p}_{12}^{(N_R)}$ holds, the solutions for $\mathbf{p}_{11}^{(m)}$ and $\mathbf{p}_{12}^{(m)}$ w.r.t. $\mathbf{H}_{21}\mathbf{p}_{11}^{(m)} = \mathbf{H}_{21}\mathbf{p}_{11}^{(N_R-1)}$ and $\mathbf{H}_{22}\mathbf{p}_{12}^{(m)} = \mathbf{H}_{22}\mathbf{p}_{12}^{(N_R)}$ alone are not available. In order to solve this problem, we let both eNBs transmit $x_1^{(m)}$ $(m = 1, \cdots, N_R - 2)$ and align the combined signal $\mathbf{H}_{21}\mathbf{p}_{11}^{(m)} + \mathbf{H}_{22}\mathbf{p}_{12}^{(m)}$ with either $\mathbf{H}_{21}\mathbf{p}_{11}^{(N_R-1)}$ or $\mathbf{H}_{22}\mathbf{p}_{12}^{(N_R)}$, so that all interferences at UE_2 are aligned in one direction.

$$\mathbf{y}_1 = \sum_{m=1}^{N_R-2} \left(\mathbf{H}_{11}\mathbf{p}_{11}^{(m)} + \mathbf{H}_{12}\mathbf{p}_{12}^{(m)} \right) x_1^{(m)} + \mathbf{H}_{11}\mathbf{p}_{11}^{(N_R-1)}x_1^{(N_R-1)} + \mathbf{H}_{12}\mathbf{p}_{12}^{(N_R)}x_1^{(N_R)} + \left(\mathbf{H}_{11}\mathbf{P}_1^{(\mathbf{s}_2)} + \mathbf{H}_{12}\mathbf{P}_2^{(\mathbf{s}_2)} \right) \mathbf{s}_2 + \mathbf{z}_1 \quad (16)$$

$$\mathbf{y}_2 = \left(\mathbf{H}_{21}\mathbf{P}_1^{(\mathbf{s}_2)} + \mathbf{H}_{22}\mathbf{P}_2^{(\mathbf{s}_2)} \right) \mathbf{s}_2 + \sum_{m=1}^{N_R-2} \left(\mathbf{H}_{21}\mathbf{p}_{11}^{(m)} + \mathbf{H}_{22}\mathbf{p}_{12}^{(m)} \right) x_1^{(m)} + \mathbf{H}_{21}\mathbf{p}_{11}^{(N_R-1)}x_1^{(N_R-1)} + \mathbf{H}_{22}\mathbf{p}_{12}^{(N_R)}x_1^{(N_R)} + \mathbf{z}_2 \quad (17)$$

TABLE I
THE ACHIEVABLE DoFs OF EACH UE UNDER VARIOUS DATA-EXCHANGE CONDITIONS.

Index	δ_1^{max}	δ_2^{max}	n_1	n_2	n_3
1	N_R	$N_R - 1$	1	1	$N_R - 1$
2	N_R	$N_R - n_1$	$n_1 \geq 1$	1	$N_R - n_1$
3	N_R	$N_R - n_1$	$n_1 \geq 1$	0	$N_R - n_1$
4	N_R	$N_R - n_2$	1	$n_2 \geq 1$	$N_R - n_2$
5	N_R	$N_R - n_2$	0	$n_2 \geq 1$	$N_R - n_2$
6	N_R	$N_R - max(1, n_1, n_2)$	n_1	n_2	$N_R - max(1, n_1, n_2)$
7	$N_R - 1$	$N_R - 1$	1	1	$N_R - 2$
8	$max(1, n_1, n_2) + n_3$	$N_R - max(1, n_1, n_2)$	n_1	n_2	n_3

Similarly to the design in previous section, all precoders can be calculated. Thus, the interferences caused by the transmission of s_2 from two eNBs to UE_2 are neutralized at UE_1, and the interferences caused by the transmission of s_{11} and s_{12} from two eNBs to UE_1 are aligned in the same direction at UE_2. ZF is then adopted to cancel the residual interference and recover the desired information. Due to space limitation, we omit design details at the receiver side which can be found in Section III. The total achievable DoFs of the given system is thus $2N_R - 1$ with the extended IAN-CoMP of which N_R data streams are for UE_1 and the other $N_R - 1$ streams for UE_2.

The system model for $M = 2$, $L = 2$, and $N_T = N_R = 2$ can be characterized by a MIMO X channel [19] whose achievable DoFs have been studied extensively. Researchers have also proposed various schemes to obtain such DoFs, in which techniques including zero-forcing, IA [20], successive decoding and dirty paper coding (DPC) [21] are employed. However, to the best of our knowledge, IN has not been considered. The achievable DoFs for a MIMO X channel where each node is equipped with N antennas increase according to $4N/3$ for no shared messages $\rightarrow 3N/2$ for partial information shared from one transmitter to the other which is feasible for downlink $\rightarrow 2N$ for full cooperation between transmitters, i.e., broadcast channels [19]. The proposed IAN-CoMP could achieve as high as $2N_R - 1$ DoFs with partial cooperation under $N_T \geq N_R$ and 2-eNB 2-UE system settings, but the overhead w.r.t. data sharing and transferring between two eNBs is high. Fortunately, we can make a flexible tradeoff between cooperation cost and achievable system DoFs. Let variables δ_1^{max}, δ_2^{max}, n_1, n_2 and n_3 denote the maximum number of data steams UE_1 and UE_2 can receive, the number of streams in s_1 exclusively sent by eNB_1 and eNB_2, and the number of data symbols in s_2 *shared* over both eNBs, respectively. Table I shows the achievable DoFs of each UE under various data-exchange conditions.

The first row of Table I indicates our extended design. From the first three rows one can see that given $n_1 \geq 1$, $n_1 \geq n_2$ and all data streams intended for UE_2 are shared over two eNBs, i.e., $\delta_2^{max} = n_3$, since interfering signals cooperatively sent by two eNBs are neutralized at UE_1, δ_1^{max} can be as large as N_R. As for UE_2, based on the discussion of Eq. (18) and Corollary 1, an n_1−dimensional space is required at UE_2 for accommodating n_1 interferences originated from eNB_1. So, the achievable DoFs of UE_2 is $\delta_2^{max} = N_R - n_1$. When $n_2 \geq 1$

and $n_2 \geq n_1$, as shown by the rows indexed from 4 to 5 in Table I, δ_1^{max} and δ_2^{max} are N_R and $N_R - n_2$, respectively. The analysis is similar to that of the first three lines. In the 6th row, the impacts of n_1 and n_2 on δ_1^{max} and δ_2^{max} are taken into account. Since the use of IA, at least one DoF is consumed at UE_2, $\delta_2^{max} = N_R - max(1, n_1, n_2)$. Line 7 shows the influence of n_3 on δ_1^{max} and δ_2^{max}. Due to the application of IA, $\delta_2^{max} = N_R - 1$. As for UE_1, n_3 data streams in s_2 are shared and cooperatively sent by both eNBs, hence achieving IN at UE_1. Then, the remaining $\delta_2^{max} - n_3$ streams intended for UE_2 will result in the same DoF cost at UE_1, yielding $\delta_1^{max} = N_R - (\delta_2^{max} - n_3)$. The last row shows general expressions of δ_1^{max} and δ_2^{max}. The achievable DoFs of the system can be easily obtained as $\delta_1^{max} + \delta_2^{max}$.

From the above discussion, we can see that in order to achieve the maximum system DoFs, i.e., $N_R + n_3$, a total of $max(1, n_1, n_2) - n_1 + 2n_3$ data streams should be shared over, or transferred between the two eNBs. Taking the design in Section III as an example where $n_1 = n_2 = 1$ and $n_3 = N_R - 1$, with $2N_R - 2$ data-exchange overhead, UE_1 and UE_2 can receive N_R and $N_R - 1$ independent streams, respectively.

B. Generalized Number of eNBs

We now generalize the number of eNBs, denoted by M, participating in CoMP. The number of UEs, L, is fixed at 2. We first present two properties of applying IA and IN in a multi-eNB multi-UE downink system as depicted in Fig. 1.

Property 1: When IA is applied once, (say) K signals are aligned in one direction at one of their unintended receivers. These interferences can be mitigated at the cost of 1 DoF, but at each of the other unintended receivers, K DoFs will be consumed.

Property 2: When IN is applied once, one interference signal can be mitigated at one of its unintended receivers without consuming any DoF, but 1 DoF is consumed at each of the other unintended receivers.

Based on Property 2, for L receivers, one-time use of IN will consume a total of $L - 2$ DoFs. Here two users are exempted from L, one of which is the intended, and the other is the undesired receiver where IN is implemented.

Using the above two properties, we can define the *cost-effectiveness ratio of interference management*, η, as the total number of DoFs consumed at all receivers divided by the number of interference signals that can be mitigated. Then, we can get:

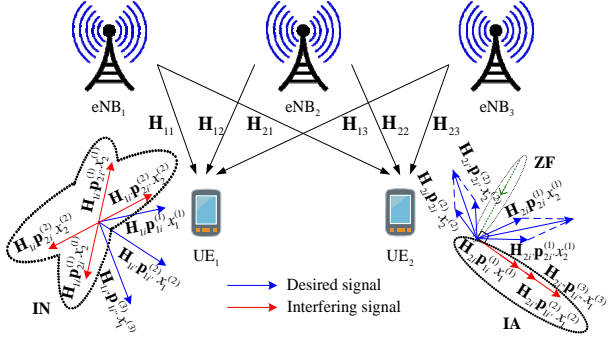$$\eta_{IA} = [1 + (L-2)K]/K, \quad \eta_{IN} = L - 2 \qquad (19)$$

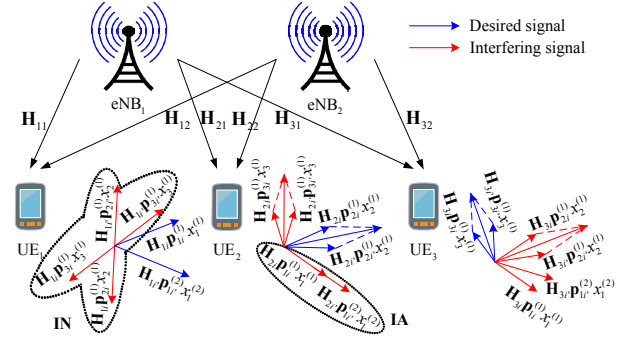Fig. 2. IAN-CoMP extension under 3-eNB and 2-UE system settings.

Fig. 3. IAN-CoMP extension under 2-eNB and 3-UE system settings.

where K is the number of aligned signals. Note that L should be at least 2 for multi-user CoMP transmission. When $L = 2$, K interferences could be mitigated at the expense of 1 DoF, so $\eta_{IA} = 1/K$. As for IN, one interference could be eliminated at no cost of DoFs, thus $\eta_{IN} = 0$. Eq. (19) shows that as L grows larger than 2, both η_{IA} and η_{IN} are greater than 1 and increase accordingly, i.e., more DoFs are consumed for interference mitigation.

In practice, IA and IN can be implemented in a *centralized* way, i.e., all signal components are aligned in one direction or paired and neutralized at a single UE; or in a *distributed* manner, i.e., alignment and neutralization of various subsets of interferences are done at multiple UEs. However, we can show that given the same set of interferences, DoF costs of both centralized IA/IN and distributed IA/IN are the same. Due to space limitation, we omit details. Without loss of generality, a centralized implementation is used in the following extension of IAN-CoMP.

Suppose $M > 2$, $L = 2$ and $N_R \geq M$, i.e., UE has sufficient antennas to decode its information. Similarly to the processing shown in Fig. 1, IN is implemented at UE_1 while IA is achieved at UE_2. The difference between $M = 2$ (Section III) and $M > 2$ lies in the fact that when $M = 2$, there are only two signal components of $\mathbf{s}_1$ which are sent by eNB_1 and eNB_2, respectively; for the other signals intended to UE_1, they are cooperatively sent by both eNBs so as to achieve alignment at UE_2. In case of $M > 2$, at most M signals could be explicitly sent by the eNBs whereas for the remainders, cooperative transmissions could be done by C_M^2 combinations of eNB-pairs. Since signals intended for UE_2, i.e., $\mathbf{s}_2$, are neutralized at UE_1, we have $\delta_1^{max} = N_R$. As for UE_2, using IA consumes 1 DoF, hence $\delta_2^{max} = N_R - 1$. So, when $M > 2$ eNBs participate in CoMP, we can achieve a selection diversity gain from multiple eNBs while keeping the total system DoFs intact. Taking system settings $M = 3$, $L = 2$, $N_R = 3$, and $N_T \geq N_R$ as an example, the proposed IAN-CoMP can be implemented as shown in Fig. 2. The extension of IAN-CoMP to more general M can be readily achieved.

In Fig. 2, the subscripts i, i' and i'' indicate the indices of eNBs, and $i \neq i' \neq i''$. As can be seen in this instance, $x_1^{(1)}$, $x_1^{(2)}$ and $x_1^{(3)}$ are sent by three eNBs, respectively, so that IA is achieved at UE_2. Moreover, $x_2^{(1)}$ and $x_2^{(2)}$ are sent from two arbitrarily selected eNB-pairs, and two corresponding signal-pairs achieve IN at UE_1 separately. As a result, we support a total of five concurrent streams, three of which are intended for UE_1 and two for UE_2.

C. Generalized Number of UEs

Here we generalize the number of simultaneously served UEs, $L > 2$. For simplicity of presentation, the number of eNBs, M is fixed at 2, and $N_R \geq M$.

We assume IN is implemented at UE_1, and IA is achieved at UE_2. According to Corollaries 2 and 3, signals achieving IN or IA at one UE cannot establish the same relationship at the other UEs. Also, based on Eq. (18), signals intended to UE_1 can be explicitly or cooperatively sent by the two eNBs so as to achieve IA at UE_2. In addition, since more CCI is introduced as L increases, the achievable DoFs of a user are dependent on those of the others. So, we get $\delta_1^{max} = N_R - (L - 1)$, $\delta_2^{max} = N_R - 1 - \sum_{l=3}^{L} \delta_l^{max}$ and $\delta_j^{max} = N_R - \sum_{l=1, l \neq j}^{L} \delta_l^{max}$ ($j = 3, \cdots, L$) where l and j are the indices of UEs. By observing the expression of δ_j^{max} ($j \geq 3$) and observing that $\delta_j^{max} \geq 1$ ($j = 1, \cdots, L$), we have:

$$\begin{cases} \sum_{l=1}^{L} \delta_l^{max} = N_R \\ \sum_{l=3}^{L} \delta_l^{max} \leq N_R - 2 \\ \sum_{l=1, l \neq j}^{L} \delta_l^{max} \leq N_R - 1, \ j = 3, \cdots, L \\ \delta_j^{max} > 0, \ j = 1, \cdots, L. \end{cases} \quad (20)$$

From the first equation in (20) we can see that when $L > 2$, the achievable system DoFs are N_R. Moreover, since $\delta_1^{max} \geq 1$, we get $L \leq N_R$. Therefore, at most $L = N_R$ users can be simultaneously supported, each being served by a single data stream.

Taking the system settings $M = 2$, $L = 3$, $N_R = 4$, and $N_T \geq N_R$ as an example, $(\delta_1^{max}, \delta_2^{max}, \delta_3^{max})$ can be selected from the set $\{(2,1,1), (1,2,1), (1,1,2)\}$ so that 4 independent data streams can be simultaneously supported. So, there could be various ways to allocate DoFs to multiple users. In practice, round-robin [22], weighted fair scheduling [23], and other channel allocation algorithms can be employed for DoFs distribution. Due to space limitation, we do not elaborate them in this paper. Fig. 3 shows the extension of IAN-CoMP under $(\delta_1^{max}, \delta_2^{max}, \delta_3^{max}) = (2,1,1)$. As can be seen, $x_1^{(1)}$ and $x_1^{(2)}$ are explicitly sent, whereas $x_2^{(1)}$ and $x_3^{(1)}$ are cooperatively sent by the two eNBs, so that IA and IN are achieved at UE_2 and UE_1, respectively. Given the other $(\delta_1^{max}, \delta_2^{max}, \delta_3^{max})$ values, the proposed IAN-CoMP can be similarly implemented.

V. EVALUATION

We now evaluate the performance of IAN-CoMP using MATLAB simulation. Fig. 4 compares the proposed scheme with five other algorithms, including ZFBF-CoMP, point-to-point (p2p) MIMO, MIMO broadcast channel (BC), IA-CoMP [9], and Non-CoMP under 2-eNB 2-UE and $N_T = N_R = 2$ system settings. For a fair comparison, we set the total system transmit power to $2P_T$, the numbers of antennas at both the transmitter and receiver sides to 4. We use the general form $[M\ L\ \Delta]$ to denote the parameter settings for different mechanisms, where M is the number of BSs, L is the number of mobile users, and Δ is the total number of data streams that can be served simultaneously for the users. For IAN-CoMP, ZFBF-CoMP, IA-CoMP and Non-CoMP, the transmit power of each eNB is P_T, each UE is equipped with $N_R = 2$ antennas, whereas for p2pMIMO and MIMO BC, there is only one BS, and hence its transmit power is $2P_T$. Moreover, for p2pMIMO, only one 4-antenna user is involved, while in MIMO BC there are two 2-antenna users. Note that with generalized parameter settings, not all the above-mentioned schemes are applicable. However, the trend of SE performance with various methods is consistent with that given in Fig. 4. For space limitation, the details are not shown in this paper.
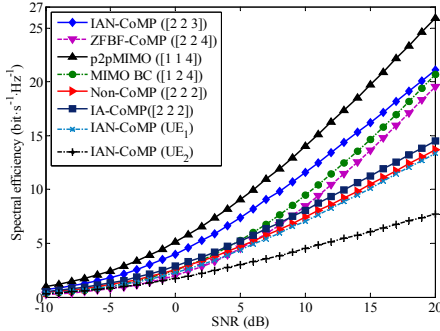

Fig. 4. SE comparison of the proposed approach with different mechanisms.

With p2pMIMO, the precoder and the receive filter are designed based on SVD, with which four orthogonal data streams can be transmitted simultaneously by exploiting spatial multiplexing. This can be regarded equivalent to the case where both eNB and UE sides ideally cooperate. As for MIMO BC, ZF-based precoding is adopted by the BS, and each user implements post-processing independently. Hence, CCI can be eliminated and four concurrent data streams are supported. With ZFBF-CoMP, complete data information and CSI are shared by eNBs, the pseudo-inverse of the matrix consisting of channels of all scheduled users is adopted as the precoder, and then four data transmissions are available. Essentially, ZFBF-CoMP is the interfering transmitter side implementation. With IA-CoMP, each transmitter can send one data stream to its receiver under the system settings. Receiver nodes decode data successively. The node which recovers its data first will forward the information to the subsequent receivers. However, the receiver side cooperation is required, which is difficult to get in the downlink. For non-CoMP, the SVD-based precoder is employed, the receive filter is designed

at each user separately for interference cancellation. Since neither the BS side nor the user side has cooperation capability, each BS serves one user with one data stream, so two streams are supported simultaneously.

As shown in Fig. 4, p2pMIMO achieves the maximum SE, since it is equivalent to the case where both BS and user sides cooperate ideally. Non-CoMP performs poorly. IA-CoMP outperforms Non-CoMP with approximately 1 bit·s^{-1}·Hz^{-1} since it exploits both coordinate transmission and receiver side cooperation. MIMO BC and ZFBF-CoMP are slightly inferior to non-CoMP in a low SNR region. Since SE is dominated by noise when SNR is low, the influence of CCI is lower than noise power. As a result, signal processing for interference elimination and suppression cannot make an obvious enhancement on the system SE, but on the contrary, effective power loss of the desired signal due to above-mentioned processing deteriorates the SE in the end. As SNR increases, interference gradually becomes the dominant factor limiting SE. Hence, SE of MIMO BC and ZFBF-CoMP improves significantly over that of non-CoMP, and approaches the proposed IAN-CoMP as SNR grows. With IAN-CoMP, interference cancellation and suppression is implemented while the strength of expected signals is maintained. Consequently, IAN-CoMP outperforms MIMO BC, ZFBF-CoMP and non-CoMP. SE of both UEs with IAN-CoMP is also plotted in Fig. 4. One can see that UE_1 achieves better transmission than UE_2 since the former is served by two data streams whereas only one is available to the latter.

Fig. 5 plots the spectral efficiency with proposed IAN-CoMP under different antenna configurations. Let the general form $[N_T\ N_R\ \Delta]$ denote the parameter settings. As shown in the figure, given $N_T \geq N_R$, the achievable SE grows as the number of antennas increases. Provided with fixed N_T (N_R), SE grows as N_R (N_T) increases. Besides, compared to N_T, increasing N_R yields more significant improvements on SE.

Fig. 6 plots the spectral efficiency of IAN-CoMP under $N_T = N_R = 2$, $L = 2$, and different Ms. SEs of both UEs are also illustrated there. Since Δ is irrelevant to M, we simply assign UE_1 with two data streams whereas UE_2 with one. As shown in the figure, both the system's SE and individual UE's grows with an increase of M, because more selection diversity gain is obtained as the number of eNBs participating in CoMP increases, which is consistent with our theoretical analysis.

Fig. 7 shows the SE performance of the proposed mechanism under different Ls. Based on the analysis in Section IV.C, the number of simultaneously supported users is limited by N_R, however, due to space limitation and hardware cost, mobile terminals cannot be equipped with a large number of antennas. In order to explicitly illustrate the impact of L on SE, we set $N_T = N_R = 5$ and $M = 2$. A general expression $[\delta_1^{max} \cdots \delta_L^{max}]$ is employed to indicate DoFs allocation to L users. Note that neutralization of all the UEs' data transmission except for UE_1's is implemented at UE_1, whereas for signals carrying UE_1's information IA is achieved at UE_2. Since severer CCI is introduced as L grows larger than 2, 2-UE case achieves the highest DoFs, thus outputting the best SE.
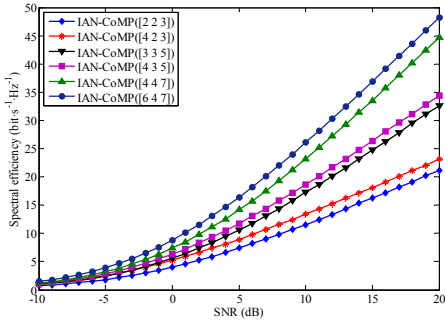
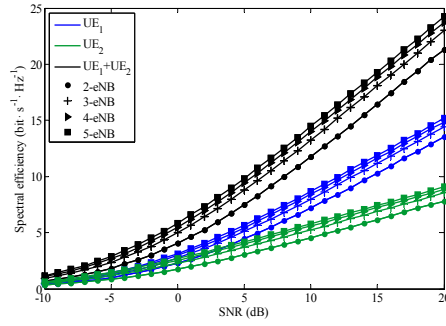Fig. 5. SE of IAN-CoMP under different N_T and N_R.

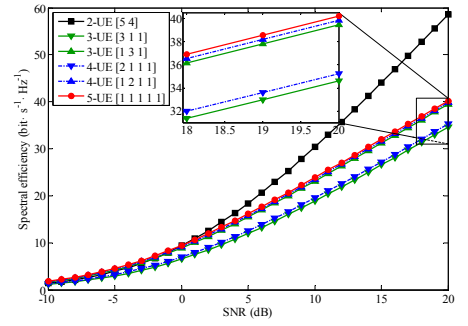Fig. 6. SE of IAN-CoMP under $N_T = N_R = 2$, $L = 2$, and different Ms.

Fig. 7. SE of IAN-CoMP under $N_T = N_R = 5$, $M = 2$, and different Ls.

Given $L > 2$ and the same system DoFs, SE improves with an increase of L since it benefits from multiple simultaneously-served users. Especially when SNR is low, such benefits may outweigh the performance loss due to severer CCI. So, the SE of 5-UE case slightly outperforms that with 2-UE under small SNR. Note that IN yields less effective signal power loss as compared to IA, resulting in higher SE, e.g., for the two 3-UE cases, the [1 3 1] DoF allocation excels the [3 1 1] case in SE, since 4 data transmissions achieve IN for the former whereas only 2 for the latter.

VI. CONCLUSION

In this paper, a new CoMP mechanism based on IAN is proposed. By exploiting the BS-side cooperation, transmit precoding and receive filtering are designed jointly. On one hand, IN is used to align two interfering signals carrying the same data in opposite directions in a subspace such that they can be canceled out. On the other hand, IA is applied to align interference signals carrying different information in the same direction in one subspace so as to reduce the dimension of received signal. Based on the cooperative preprocessing at eNBs, ZF is employed at the receiver side to cancel the residual interference and recover the desired information. This scheme is designed first under a specific system configuration, and then extended to more general cases. The proposed IAN-CoMP could achieve effective interference cancellation and suppression by exploiting limited cooperation, hence improving spectral efficiency for cell-edge users significantly.

REFERENCES

[1] G. Y. Li, Z. Xu, C. Xiong, et al., "Energy-efficient wireless communications: Tutorial, survey, and open issues," IEEE Wireless Commun. Mag., vol. 18, no. 6, pp. 28-35, 2011.
[2] 3GPP TR36.814, "Further advancements for E-UTRA physical layer aspects; Coordinated multiple point transmission and reception," 2010.
[3] P. Marsch, G. P. Fettweis, "Coordinated multi-point in mobile communications: From theory to practice," Cambridge Univ. Press, 2011.
[4] W. Liu, S. Han, C. Yang, "Hybrid cooperative transmission in heterogeneous networks," in Proc. of the IEEE Int. Sympo. on Personal Indoor and Mobile Radio Commun. (PIMRC), pp. 921-925, 2012.
[5] S. Han, C. Yang, M. Bengtsson, et al., "Channel norm-based user scheduler in coordinated multi-point systems," in Proc. of the IEEE Global Commun. Conf. (GLOBECOM), pp. 1-5, 2009.
[6] Q. Zhang, C. Yang, "Semi-dynamic mode selection in base station cooperative transmission system," in Proc. of the IEEE Vehicular Technology Conf. (VTC), pp. 1-5, 2011.
[7] C. M. Yetis, T. Gou, S. A. Jafar, et al., "On feasibility of interference alignment in MIMO interference networks," IEEE Trans. Sig. Process., vol. 58, no. 9, pp. 4771-4782, 2010.
[8] C. Na, X. Hou, A. Harada, "Two-cell coordinated transmission scheme based on interference alignment and MU-MIMO beamforming," in Proc. of the IEEE Vehicular Technology Conf. (VTC), pp. 1-5, 2012.
[9] S. M. Razavi, T. Ratnarajah, "Interference alignment in partially coordinated multipoint receivers," in Proc. of the IEEE Int. Sympo. on Personal Indoor and Mobile Radio Commun. (PIMRC), pp. 1114-1118, 2013.
[10] J. Chen, A. Singh, P. Elia, et al., "Interference neutralization for separated multiuser uplink-downlink with distributed relays," in Proc. of the Inf. Theory and Applications Workshop (ITA), pp. 1-9, 2011.
[11] T. Gou, S. A. Jafar, C. Wang, et al., "Aligned interference neutralization and the degrees of freedom of the 2×2×2 interference channel," IEEE Trans. Inf. Theory, vol. 58, no. 7, pp. 4381-4395, 2012.
[12] N. Lee, C. Wang, "Aligned interference neutralization and the degrees of freedom of the two-user wireless networks with an instantaneous relay," IEEE Trans. Commun., vol. 61, no. 9, pp. 3611-3619, 2013.
[13] Z. Ho, E. A. Jorswieck, "Instantaneous relaying: optimal strategies and interference neutralization," IEEE Trans. Sig. Process., vol. 60, no. 12, pp. 6655-6668, 2012.
[14] S. A. Jafar, S. Shamai, "Degrees of freedom region of the MIMO X channel," IEEE Trans. Inf. Theory, vol. 54, no. 1, pp. 151-170, 2008.
[15] V. Jungnickel, K. Manolakis, S. Jaeckel, et al., "Backhaul requirements for inter-site cooperation in heterogeneous LTE-Advanced networks," in Proc. of the IEEE Int. Conf. on Commun. (ICC), pp. 905-910, 2013.
[16] I. F. Akyildiz, D. M. Gutierrez-Estevez, R. Balakrishnan, E. Chavarria-Reyes, "LTE-Advanced and the evolution to Beyond 4G (B4G) systems," Physical Communication, vol. 10, pp. 31-60, 2014.
[17] S. Gollakota, S. D. Perli, D. Katabi, "Interference alignment and cancellation," in Proc. of the ACM SIGCOMM Conf. on Data Commun. (SIGCOMM), pp. 159-170, 2009.
[18] Z. Li, B. Shen, J. Li, "Interference alignment and cancellation based concurrent transmission and scheduling scheme for multiuser CR-MIMO system," China communications, vol. 10, no. 8, pp. 36-43, 2013.
[19] S. A. Jafar, S. Shamai, "Degrees of freedom region of the MIMO X channel," IEEE Trans. Inf. Theory, vol. 54, no. 1, pp. 151-170, 2008.
[20] M. A. Maddah-Ali, A. S. Motahari, A. K. Khandani, "Communication over MIMO X channels: interference alignment, decomposition, and performance analysis," IEEE Trans. Inf. Theory, vol. 54, no. 8, pp. 3457-3470, 2008.
[21] M. A. Maddah-Ali, A. S. Motahari, A. K. Khandani, "Signaling over MIMO multi-base systems: combination of multi-access and broadcast schemes," in Proc. of the IEEE Int. Sympo. on Inf. Theory (ISIT), pp. 2104-2108, 2006.
[22] C. Simon, G. Leus, "Round-robin scheduling for orthogonal beamforming with limited feedback ," IEEE Trans. Wireless Commun., vol. 10, no. 8, pp. 2486-2496, 2011.
[23] M. Mehrjoo, M. K. Awad, M. Dianati, Xuemin Shen, "Design of fair weights for heterogeneous traffic scheduling in multichannel wireless networks," IEEE Trans. Commun., vol. 58, no. 10, pp. 2892-2902, 2010.